Hydrodynamic interactions in topologically linked ring polymers

Phillip M. Rauscher,[1] Stuart J. Rowan,[1,2,3,4] and Juan J. de Pablo[1,4,5,*]

[1]*Pritzker School of Molecular Engineering, University of Chicago, Chicago, Illinois 60637, USA*
[2]*Department of Chemistry, University of Chicago, Chicago, Illinois 60637, USA*
[3]*Chemical Sciences and Engineering Division, Argonne National Laboratory, Lemont, Illinois 60439, USA*
[4]*Center for Molecular Engineering, Argonne National Laboratory, Lemont, Illinois 60439, USA*
[5]*Materials Science Division, Argonne National Laboratory, Lemont, Illinois 60439, USA*

(Received 15 July 2020; accepted 21 August 2020; published 22 September 2020)

Despite decades of interdisciplinary research on topologically linked ring polymers, their dynamics remain largely unstudied. These systems represent a major scientific challenge as they are often subject to both topological and hydrodynamic interactions (HI), which render dynamical solutions either mathematically intractable or computationally prohibitive. Here we circumvent these limitations by preaveraging the HI of linked rings. We show that the symmetry of ring polymers leads to a hydrodynamic decoupling of ring dynamics. This decoupling is valid even for nonideal polymers and nonequilibrium conditions. Physically, our findings suggest that the effects of topology and HI are nearly independent and do not act cooperatively to influence polymer dynamics. We use this result to develop highly efficient Brownian dynamics algorithms that offer enormous performance improvements over conventional methods and apply these algorithms to simulate catenated ring polymers at equilibrium, confirming the independence of topological effects and HI. The methods developed here can be used to study and simulate large systems of linked rings with HI, including kinetoplast DNA, Olympic gels, and poly[*n*]catenanes.

DOI: 10.1103/PhysRevE.102.032502

I. INTRODUCTION

The dynamical interplay between polymer topology and hydrodynamic interactions (HI) has been a topic of considerable interest [1], particularly within the context of unknotted [2–11] and knotted [12–16] ring polymers. In contrast, the dynamics of *linked* rings in solution has received limited attention [17], despite being a fixture of the biophysics literature for decades [18–21] and a frequent target of chemists [22,23]. Recent simulations have shown that the dynamics of these systems exhibit pronounced topological effects [24], even within single polymers [25]. In particular, the dynamics of linked rings are considerably slower than their unlinked counterparts, a result that appears to hold for all ring sizes, suggesting that the topological constraints act on the length scale of the entire ring. However, only rings of moderate size have been characterized thus far, and only Kanaeda and Deguchi [26] have studied such systems with HI. Even then, only the diffusion coefficient of very small catenanes was considered, leaving important questions unaddressed. For instance, dynamical scaling relations for these systems have not yet been firmly established, and it is not clear how (or if) topological interactions and HI act cooperatively to influence ring dynamics. These same questions are also important in larger interlocked systems such as kinetoplasts [27,28] and Olympic gels [29], which have attracted attention in recent years.

Here we use theory and Brownian dynamics (BD) simulations to investigate the dynamics of linked ring polymers with HI. These systems present two major challenges: (1) HI and topological effects render the equations of motion analytically intractable, and (2) numerical simulations are highly computationally demanding. We address the former by using averaged HI [30] and show that the symmetries of ring molecules greatly simplify the situation. Physically, this result suggests that the effects of topology and HI are roughly independent. It also allows us to tackle the computational challenge by designing highly efficient BD algorithms, which we use to simulate catenated ring polymers at equilibrium to validate the theoretical predictions. From a theoretical perspective, our results demonstrate how the symmetries of ring polymer systems can be used to simplify otherwise intractable problems. Meanwhile, the algorithms developed here enable efficient simulations of large interlocked polymer systems with HI.

II. THEORY

Consider a group of n linked ring polymers, each comprising m identical interacting Brownian particles, containing $N = n \times m$ particles in total. We assume that there are no disconnected (or free) rings. Using the bead radius a, the thermal energy k_BT, and the bead diffusion time $\tau_0 = 6\pi\eta a^3/k_BT$ (with η the solvent viscosity) as the units of length, energy, and time, respectively, the dynamics of the particles at equilibrium are described by the dimensionless Langevin equation [31]:

$$\frac{d\boldsymbol{R}}{dt} = -\boldsymbol{H}\cdot\frac{\partial U}{\partial \boldsymbol{R}} + \sqrt{2}\boldsymbol{B}\cdot d\boldsymbol{W}, \tag{1}$$

*depablo@uchicago.edu

where $\boldsymbol{R}$ is a vector of particle positions, $\boldsymbol{H}$ is the $N \times N$ mobility or hydrodynamic interaction (HI) matrix whose elements $\boldsymbol{H}_{ij}$ are tensors that describe the direction-dependent hydrodynamic coupling between beads i and j, U is the system interaction potential, $d\boldsymbol{W}$ is an increment of the Wiener process, and $\boldsymbol{B}\boldsymbol{B}^T = \boldsymbol{H}$ per the fluctuation-dissipation theorem. Normally, a divergence term of the form $\partial/\partial\boldsymbol{R} \cdot \boldsymbol{H}$ is included in Eq. (1), but this will be neglected as it does not affect our results (see Supplemental Material [32]) and vanishes due to solvent incompressibility for many commonly employed forms of $\boldsymbol{H}_{ij}$ (e.g., Oseen-Burgers [31], Rotne-Prager-Yamakawa [36,37], and Zylka-Öttinger [38] tensors).

Equation (1) represents a set of coupled, nonlinear equations since both $\boldsymbol{H}$ and the forces $(-\partial U/\partial \boldsymbol{R})$ depend on the particle positions. Zimm [30] replaced $\boldsymbol{H}$ with its equilibrium average, $\langle \boldsymbol{H} \rangle_{\text{eq}}$, thereby simplifying the mathematical treatment of mobility. The success of these "preaveraged" HI [39] inspired the closely related "consistently averaged" HI under nonequilibrium conditions [40–42] and "iterative averaging" for simulations [4]. In general, these methods are most appropriate when conformational fluctuations are negligible, typically at or near equilibrium. Here we follow this well-established family of approximations and study the dynamical consequences in the context of catenated polymers.

To begin, we establish a useful indexing convention: the vector $\boldsymbol{R}$ is broken up into blocks of size m, each of which represents the position of the beads within a single ring, denoted $\boldsymbol{R}^\alpha$ with $\alpha = 1, 2, \ldots, n$. Following this convention, $\boldsymbol{H}$ may be written as a $n \times n$ block matrix with each $m \times m$ block $\boldsymbol{H}^{\alpha\beta}$ representing the HI between the beads on rings α and β. The on-diagonal blocks represent the coupling between beads on the same ring polymer, while the off-diagonal blocks represent the coupling between beads on different rings.

We now consider the equilibrium average of the mobility matrix, $\langle \boldsymbol{H} \rangle$ (the subscript "eq" has been dropped for brevity). The elements $\langle \boldsymbol{H}_{ij} \rangle$ depend on the details of the system, e.g., chemical composition, solvent, m, etc., and must be determined by simulation except for simple models. However, for the time being, we are not concerned with the value(s) of $\langle \boldsymbol{H} \rangle$, but rather with its mathematical structure. In particular, the form of the averaged blocks $\langle \boldsymbol{H} \rangle^{\alpha\beta}$ is constrained by continuous symmetries: all particles within ring polymers are statistically identical. Since the indexing of beads is therefore arbitrary, each row in a given block $\langle \boldsymbol{H} \rangle^{\alpha\beta}$ is identical to the other rows but for a shift in indices; in mathematical terms, the blocks are circulant [43]. The eigenvectors of circulant matrices are simply the Fourier modes $\boldsymbol{\omega}_q = \boldsymbol{\delta}/\sqrt{m}(1, w_q, w_q^2, \ldots, w_q^{m-1})$ where $\boldsymbol{\delta}$ is the identity tensor, $q = 0, 1, \ldots, m-1$, $w_q = \exp(2\pi i q/m)$ and $i = \sqrt{-1}$, suggesting a convenient coordinate basis for the system.

The off-diagonal blocks $\langle \boldsymbol{H} \rangle^{\alpha\beta} (\alpha \neq \beta)$ have even greater symmetry. Since the average must not depend on the indexing of *either* ring, all elements are equal:

$$\langle \boldsymbol{H} \rangle^{\alpha\beta} = \frac{\boldsymbol{h}_0^{\alpha\beta}}{m} \begin{bmatrix} 1 & 1 & \cdots & \\ 1 & 1 & & \\ \vdots & & \ddots & \\ & & & 1 \end{bmatrix} \equiv \frac{\boldsymbol{h}_0^{\alpha\beta}}{m} \mathbf{1} \quad (\alpha \neq \beta), \tag{2}$$

where we have defined the $m \times m$ "ones" matrix $\mathbf{1}$ in the second equality and the factor $1/m$ is included for later normalization.

Having determined the form of $\langle \boldsymbol{H} \rangle$, we can now diagonalize each of its blocks using the Fourier modes. Denoting by $\boldsymbol{\omega}$ the $m \times m$ matrix whose columns are given by the modes $\boldsymbol{\omega}_q$, we define the orthonormal block-diagonal matrix $\boldsymbol{\Omega} \equiv \boldsymbol{\omega} \otimes \boldsymbol{I}_n$, where $\boldsymbol{I}_n$ is the $n \times n$ identity matrix. The matrix $\boldsymbol{\Omega}$ will be used to transform Eq. (1). Before continuing, it is important to make a key observation: the Fourier modes are physically equivalent to the Rouse modes for ring polymers [43–45]. For ring α, we have $\boldsymbol{X}^\alpha = \boldsymbol{\omega}^\dagger \boldsymbol{R}^\alpha$. Accordingly, the mode $q = 0$ corresponds to the ring center-of-mass (CM) position while the modes $q > 0$ describe the internal configuration of the polymer.

Substituting $\langle \boldsymbol{H} \rangle$ into Eq. (1) and multiplying by $\boldsymbol{\Omega}^\dagger$, we have

$$\frac{d\boldsymbol{X}}{dt} = -\widehat{\boldsymbol{H}} \cdot \frac{\partial U}{\partial \boldsymbol{X}} + \sqrt{2}\widehat{\boldsymbol{B}} \cdot d\boldsymbol{Z}, \tag{3}$$

where $\widehat{\boldsymbol{H}} = \boldsymbol{\Omega}^\dagger \langle \boldsymbol{H} \rangle \boldsymbol{\Omega}$, $\widehat{\boldsymbol{B}} = \boldsymbol{\Omega}^\dagger \langle \boldsymbol{B} \rangle \boldsymbol{\Omega}$, and $d\boldsymbol{Z} = \boldsymbol{\Omega}^\dagger d\boldsymbol{W}$. The fluctuation-dissipation theorem and the orthonormality of $\boldsymbol{\Omega}$ imply $\widehat{\boldsymbol{B}}\widehat{\boldsymbol{B}}^T = \widehat{\boldsymbol{H}}$.

We now consider the form of $\widehat{\boldsymbol{H}}$, which inherits the block structure of $\boldsymbol{H}$. The on-diagonal blocks $\widehat{\boldsymbol{H}}^{\alpha\alpha}$ are themselves diagonal with elements given by the eigenvalues of $\langle \boldsymbol{H} \rangle^{\alpha\alpha}$, denoted $\boldsymbol{h}_q^{\alpha\alpha}$ with $q = 0, 1, \ldots, m-1$. This result indicates that in the preaveraging approximation, the various internal modes of the rings do not hydrodynamically couple to one another [43].

To determine the form of the off-diagonal blocks of $\widehat{\boldsymbol{H}}$, we first calculate $\boldsymbol{\omega}^T \mathbf{1} \boldsymbol{\omega} = m\boldsymbol{\delta}\boldsymbol{C}$ where $\boldsymbol{C}$ is the $m \times m$ "corner" matrix with elements $C_{ij} = \delta_{i1}\delta_{j1}$, so-called because only the upper-left element is nonzero. Using this result along with Eq. (2), we obtain

$$\widehat{\boldsymbol{H}} = \begin{bmatrix} \widehat{\boldsymbol{H}}^{11} & \boldsymbol{h}_0^{12}\boldsymbol{C} & \cdots & \\ \boldsymbol{h}_0^{12}\boldsymbol{C} & \widehat{\boldsymbol{H}}^{22} & & \\ \vdots & & \ddots & \\ & & & \widehat{\boldsymbol{H}}^{nn} \end{bmatrix}. \tag{4}$$

We again emphasize that the on-diagonal blocks $\widehat{\boldsymbol{H}}^{\alpha\alpha}$ are diagonal. The matrix $\widehat{\boldsymbol{B}}$ can also be written in a similar manner with diagonal on-diagonal blocks $\widehat{\boldsymbol{B}}^{\alpha\alpha}$ having nonzero entries $\boldsymbol{b}_q^{\alpha\alpha}$ $(q = 0, 1, \ldots, m-1)$ and off-diagonal blocks $\boldsymbol{b}_0^{\alpha\beta}\boldsymbol{C}$ (see Supplemental Material [32]). From Eq. (4), the elements of the off-diagonal matrices, which represent HI between modes on different rings, all vanish except those which describe coupling between the "zeroth" modes. But as discussed above, these modes simply correspond to the ring CMs. Using this result, Eq. (3) can be separated into two sets of equations: one for the CM modes $\boldsymbol{X}_0^\alpha$ and another for the intraring modes, $\boldsymbol{X}_q^\alpha$ $(q > 0)$:

$$\frac{d\boldsymbol{X}_0^\alpha}{dt} = \sum_{\beta=1}^{n} \left\{ -\boldsymbol{h}_0^{\alpha\beta} \frac{\partial U}{\partial \boldsymbol{X}_0^\beta} + \sqrt{2}\boldsymbol{b}_0^{\alpha\beta} d\boldsymbol{Z}_0^\beta \right\}, \tag{5a}$$

$$\frac{d\boldsymbol{X}_q^\alpha}{dt} = -\boldsymbol{h}_q^{\alpha\alpha} \frac{\partial U}{\partial \boldsymbol{X}_q^\alpha} + \sqrt{2}\boldsymbol{b}_q^{\alpha\alpha} d\boldsymbol{Z}_q^\alpha. \tag{5b}$$

Thus, by a combination of preaveraging and choosing a suitable coordinate basis, the set of nm coupled vector equations, Eq. (1), has been reduced to n coupled equations and $n(m-1)$ (hydrodynamically) independent ones.

According to Eq. (5b), the internal dynamics of the rings ($q > 0$) are *hydrodynamically decoupled* from one another: the only direct coupling between rings exists at the coarse CM level, Eq. (5a). In essence, topology and HI do not act cooperatively to influence the ring dynamics, at least in a direct sense. Of course, the dynamics of the rings will still be coupled through the forces ($-\partial U/\partial \boldsymbol{X}$), but these primarily reflect the topological constraints; hydrodynamic contributions are higher-order effects (see below). This result is particularly striking as it does not actually require that the average be taken over the *equilibrium* distribution. Rather, the decoupling was obtained purely on the basis of symmetries in the rings, which still exist even in nonideal (non-Gaussian) polymers or in nonequilibrium conditions. In such cases, Eqs. (5) still hold, but with generally anisotropic tensors $\boldsymbol{h}^{\alpha\beta}$ and $\boldsymbol{b}^{\alpha\beta}$. In addition, the precise details of the topological linking do not affect the result, which should therefore hold for arbitrary link complexity.

Since there is no *direct* coupling between topology and HI, we now turn our attention to how the two may couple *indirectly*. Equations (5) suggest two mechanisms. First, the values $\boldsymbol{h}_q^{\alpha\alpha}$ may be altered by topological constraints. While this is likely important far from equilibrium, it is negligible for simple links in equilibrium (see Supplemental Material [32]). Second, the non-local-in-time force correlations between modes or segments (which are sensitive to topology) are modified, either by deviations of $\boldsymbol{h}_q^{\alpha\alpha}$ from the freely draining value(s), $\boldsymbol{\delta}$, or by ring CM dynamics, which are still hydrodynamically correlated via Eq. (5a). These effects are expected to be small, as they describe how the force on a given mode is affected by changes in the dynamics of *other* modes at *earlier* times. The small magnitude of the indirect coupling, and the absence of a direct coupling, indicate that topology and HI are pseudo-independent, provided the averaging approximation is valid.

If topology and HI were in fact independent, the consequences of topological linking would be comparable for systems with and without HI. In the remainder of this paper, we develop and apply Brownian dynamics simulations to test this result and quantify the importance of the higher-order effects described above. Before continuing, we note that although the theory and methods presented here were developed in the context of linked ring polymers, they are equally valid for isolated or knotted ring polymers.

III. METHODS AND ALGORITHMS

Equations (5) suggest an efficient scheme for BD simulations, in which the forces are calculated in real space, while the particle positions are updated in the Fourier mode representation. The advantage of this approach is that the products $\boldsymbol{H}\cdot\partial U/\partial \boldsymbol{R}$ and $\boldsymbol{B}\cdot d\boldsymbol{W}$ required for integrating Eq. (1) [typically $O(N^2)$ operations] are no longer necessary in integrating Eqs. (5), where such products are only needed for the CM modes. Thus, the position update is split into a $O(nm)$ operation for modes $q > 0$ and a $O(n^2)$ operation for modes $q = 0$. Of course, one must constantly transform back-and-forth between the real-space and Fourier-space representations, but with fast Fourier transforms the scaling of these operations is only $O(nm\log m)$. As a result, this algorithm provides substantial improvements in computational performance compared to typical conformationally averaged simulations [4]. For the largest systems studied here (see below), the performance is improved by over an order of magnitude [32].

For systems with large conformational fluctuations, averaged HI may not provide qualitatively correct results. However, the algorithm above can be modified such that some time-dependent variation in HI is preserved. At each time step, the time-dependent HI matrix $\boldsymbol{H}(t)$ is calculated and each of the on-diagonal blocks $\boldsymbol{H}^{\alpha\alpha}(t)$ is averaged along its diagonals, such that it becomes circulant. The off-diagonal blocks $\boldsymbol{H}^{\alpha\beta}(t)$ ($\alpha \neq \beta$) are then averaged over all elements to obtain the form of Eq. (2). Moving to the Fourier space, the time-dependent matrix $\widehat{\boldsymbol{H}}(t)$ will again have the form of Eq. (4), and $\widehat{\boldsymbol{B}}(t)$ may be computed with complexity $O(nm) + O(n^3)$ (see Supplemental Material [32]). The remainder of the algorithm is identical to that described above. In general, the interring couplings $\boldsymbol{h}_0^{\alpha\beta}$ and the intraring eigenvalues $\boldsymbol{h}_q^{\alpha\alpha}$ are not isotropic tensors. However, as discussed before, this anisotropy does not invalidate the hydrodynamic decoupling in Eqs. (5).

Unlike the preaveraged matrix $\langle\boldsymbol{H}\rangle$, the time-dependent "instantaneously averaged" matrix $\widehat{\boldsymbol{H}}(t)$ still contains some information regarding the polymer conformation at any given moment in time and may therefore capture the effects of large-scale conformational fluctuations with minimal computational expense. Moreover, the equilibrium-averaged matrix $\langle\boldsymbol{H}\rangle$ need not be known beforehand. These advantages make instantaneously averaged HI well suited to nonequilibrium BD simulations. The two algorithms described above are presented more formally in the Supplemental Material [32]. Note that both methods include the mechanisms of indirect HI-topology coupling described earlier. Since these algorithms are considerably more efficient than ordinary BD simulations, they can be used to study large, complex interlocked materials, such as kinetoplasts, Olympic gels, or poly[n]catenanes [23] with HI both at equilibrium and nonequilibrium conditions. A sample code implementing these algorithms in the Python programming language [46] is available online [47].

To test the theoretical results presented above, we have conducted BD simulations of unlinks ($n = 1$) and Hopf links (i.e., [2]catenanes, $n = 2$) in equilibrium at theta-solvent conditions. We consider ring sizes of $m = 16$, 32, 48, 64, 96, 128, 256, and 512 and include HI at four different levels: freely draining (no HI), full HI (typical BD simulation), and pre- and instantaneously averaged HI (see above); see Supplemental Material [32] for details. For the systems with full HI, only ring sizes up to $m = 96$ could be simulated owing to the considerable computational demands; only with the more efficient algorithms developed above can the larger systems be simulated with HI.

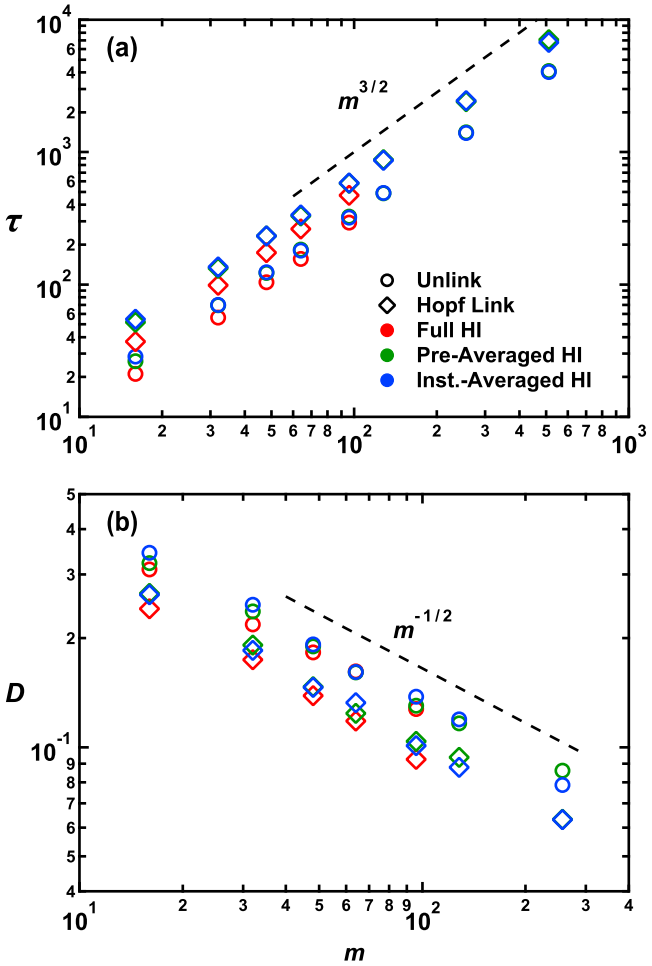

FIG. 1. (a) Longest ring relaxation times, τ, and (b) diffusion coefficients, D, for linked and unlinked ring polymers as a function of ring size, m, with various levels of HI. Error bars are approximately the size of the data points. Dashed lines indicate the Zimm scaling predictions.

IV. RESULTS AND DISCUSSION

We focus on the long-time, large-length-scale dynamics, as these are the most sensitive to topological effects [24,25]. In particular, we examine the longest relaxation times of the individual rings (τ, determined from the autocorrelation function of the lowest Rouse mode) and the diffusion coefficient of the whole polymer assembly (D, determined by linear regression on the CM mean-squared displacement), shown in Fig. 1.

We begin by assessing the validity of the averaging approximations, i.e., how well pre- and instantaneous averaging reproduce the correct values of τ and D. At small m, the averaging algorithms show considerable deviations in τ compared to the full HI simulations. However, as m increases, these deviations are reduced and are only about 10% by the time $m = 96$, comparable to the statistical uncertainty in the results. In general, D shows better agreement, exhibiting differences of only 5%–10% throughout the range of m values.

Despite these differences, all data show the same scaling behavior. Zimm theory predicts $\tau \sim R_{g,r}^3$ and $D \sim R_g^{-1}$ [39]

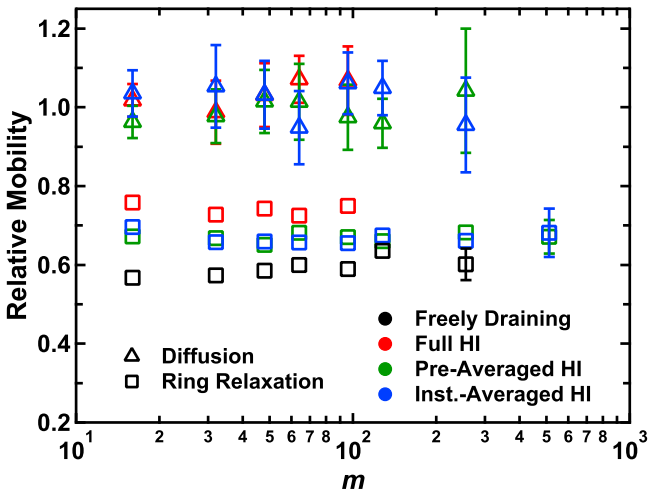

FIG. 2. Relative mobility of Hopf links and unlinks as calculated from either the diffusion coefficient or the ring relaxation times (see main text for details). Error bars are roughly the size of the data points, except where explicitly shown.

where R_g is the polymer radius of gyration and $R_{g,r}$ is the radius of gyration of an individual ring (for unlinked rings, these are identical). Since our systems are near the theta point, we expect $R_g \sim R_{g,r} \sim m^{1/2}$ and therefore $\tau \sim m^{3/2}$ and $D \sim m^{-1/2}$. This is indeed the case for all algorithms used, as shown in Fig. 1.

We now quantify the effects of topological linking on the system dynamics. As in previous works, the relaxation times of the rings are increased by the presence of threading segments [24,25]. However, this is expected since topological linking also causes the rings to swell relative to the unlinked state [25,48,49], which should increase the relaxation times according to the scaling relations above. Meanwhile, the increased mass and overall size of the Hopf links compared to the unlinks will naturally favor smaller diffusion coefficients; this effect is also observed in the simulation data.

To understand whether the topology-dependent dynamical properties are simply the result of changes in ring size, we introduce effective mobilities $\mu_\tau(\mathcal{T}) \equiv R_{g,r}^3/\tau$ and $\mu_D(\mathcal{T}) \equiv (R_g D)^{-1}$ where $\mathcal{T}$ represents the topological state of the rings, either unlinks, $\mathcal{U}$, or Hopf links, $\mathcal{H}$. According to the scaling predictions above, these mobilities should be independent of m but may still depend on $\mathcal{T}$. To isolated and quantify topological effects, we consider the *ratios* of the effective mobilities, $\mu_\tau(\mathcal{H})/\mu_\tau(\mathcal{U})$ and $\mu_D(\mathcal{H})/\mu_D(\mathcal{U})$, which we dub *relative* mobilities.

In a similar manner, we wish to assess whether topological effects are manifested differently in the presence of HI to test the theoretical results presented above. To do so, we note that without HI, relaxation times scale as $\tau \sim mR_{g,r}^2$ [39], suggesting an effective mobility $\mu_0(\mathcal{T}) \equiv mR_{g,r}^2/\tau$. As above, the relative mobility $\mu_0(\mathcal{H})/\mu_0(\mathcal{U})$ is the quantity of interest. Note that any mobility calculated from D in freely draining systems is not meaningful, as these systems have $D = 1/N$ identically, regardless of polymer architecture or topology.

The relative mobilities are shown in Fig. 2. As expected, these data are essentially independent of m. The values calculated from D are approximately unity for all algorithms,

suggesting that the overall motion of the polymer is controlled primarily by its size, so topological effects are only important insofar as they affect polymer dimensions. However, in freely draining systems, the relative mobility calculated from τ is on average $\sim$0.6 due to topological effects, in agreement with previous results [24,25]. In the presence of full HI, the relative mobility is slightly larger, $\sim$0.74, suggesting that there is indeed some coupling between topology and HI. Nevertheless, this difference is surprisingly modest, given how dramatically both HI and topology alter polymer dynamics. Furthermore, when the higher-order, indirect effects are included through pre- and instantaneously averaged HI, much of this difference is eliminated, with relative mobilities of $\sim$0.67.

The remaining discrepancy between the relative mobilities of averaged and full HI represents the *direct* coupling of topology and HI. This coupling is likely caused by the heterogeneous hydrodynamic environment of the systems. HI effectively "shield" segments from solvent drag forces; the more beads nearby, the more shielding and the faster the segmental dynamics. Averaging procedures neglect any heterogeneity in this shielding, which breaks the symmetry of the rings such that the Fourier modes are not truly hydrodynamically decoupled. The data in Fig. 1 suggest that this approximation leads to some errors even in the case of unlinked ring polymers. These discrepancies may be exacerbated in Hopf links, where segments on the same polymer may be either surrounded by the beads of the linked ring or distantly separated from them. This may explain why simulations with averaged HI exhibit poorer agreement for Hopf links versus unlinks (Fig. 1). Nevertheless, the relative mobilities are still quite close to one another, differing by just $\sim$10%, and supporting the theoretical result that there is little *direct* coupling between topology and HI and that the two effects are pseudo-independent at equilibrium.

V. CONCLUSIONS

This work represents a first step in the study of the dynamics of topologically linked polymers in solution. We have shown that by leveraging the symmetries inherent to ring polymers, the effects of topology and HI may be considered approximately independently. Furthermore, we have developed efficient Brownian dynamics algorithms which allow for simulations of large interlocking polymer systems and long timescales. Taken together, these advances have brought us into a position from which to pose and answer a range of questions concerning the dynamics of linked ring polymers in solution that could not be addressed before.

ACKNOWLEDGMENTS

We gratefully acknowledge A. M. Rumyantsev, N. E. Jackson, and H. C. Öttinger for helpful discussions and comments. This work was supported by the Department of Energy, Office of Science, Basic Energy Sciences, Division of Materials Science and Engineering. Early investigations of catenated polymer systems were also supported by the National Science Foundation (NSF) under Grants No. CHE-1402849 and No. CHE-1903603. The development of materials for impact mitigation, of which interlocked polymers are a category, is supported by the National Institute of Standards and Technology (NIST) through the Center for Hierarchical Materials Design (CHiMaD). P.M.R. thanks the NSF for the award of a Graduate Research Fellowship, Grant No. 1746045. Any opinions, findings, and conclusions or recommendations expressed in this material are those of the author(s) and do not necessarily reflect the views of the NSF.

[1] D. J. Mai and C. M. Schroeder, Curr. Opin. Colloid Interface Sci. **26**, 28 (2016).
[2] N. Kanaeda and T. Deguchi, J. Phys. A: Math. Theor. **41**, 145004 (2008).
[3] K. W. Hsiao, C. M. Schroeder, and C. E. Sing, Macromolecules **49**, 1961 (2016).
[4] L. Miao, C. D. Young, and C. E. Sing, J. Chem. Phys. **147**, 024904 (2017).
[5] B. W. Soh, A. R. Klotz, R. M. Robertson-Anderson, and P. S. Doyle, Phys. Rev. Lett. **123**, 048002 (2019).
[6] M. Handa and P. Biswas, Soft Matter **15**, 5896 (2019).
[7] Z. Wang, Q. Zhai, W. Chen, X. Wang, Y. Lu, and L. An, Macromolecules **52**, 8144 (2019).
[8] M. Liebetreu and C. N. Likos, Commun. Materials **1**, 4 (2019).
[9] C. D. Young, J. R. Qian, M. Marvin, and C. E. Sing, Phys. Rev. E **99**, 062502 (2019).
[10] K. R. Peddireddy, M. Lee, Y. Zhou, S. Adalbert, S. Anderson, C. M. Schroeder, and R. M. Robertson-Anderson, Soft Matter **16**, 152 (2019).
[11] M. Gruziel-Słomka, P. Kondratiuk, P. Szymczak, and M. L. Ekiel-Jeżewska, Soft Matter **15**, 7262 (2019).
[12] N. Kanaeda and T. Deguchi, Phys. Rev. E **79**, 021806 (2009).
[13] M. Liebetreu, M. Ripoll, and C. N. Likos, ACS Macro Lett. **7**, 447 (2018).
[14] B. W. Soh, A. R. Klotz, and P. S. Doyle, Macromolecules **51**, 9562 (2018).
[15] M. Gruziel, K. Thyagarajan, G. Dietler, A. Stasiak, M. L. Ekiel-Jezewska, and P. Szymczak, Phys. Rev. Lett. **121**, 127801 (2018).
[16] L. B. Weiss, M. Marenda, C. Micheletti, and C. N. Likos, Macromolecules **52**, 4111 (2019).
[17] Throughout this paper, the term "linked rings" refers to mathematical links. In other words, the rings are *topologically* bound to one another (or interlocked) with no covalent or other permanent attachment.
[18] M. D. Frank-Kamenetskii, A. V. Lukashin, and A. V. Vologodskii, Nature (London) **258**, 398 (1975).
[19] K. N. Kreuzer and N. R. Cozzarelli, Cell **20**, 245 (1980).
[20] S. M. Mirkin, in *Encyclopedia of Life Sciences* (John Wiley & Sons, Chichester, UK, 2001).
[21] A. Vologodskii and V. V. Rybenkov, Phys. Chem. Chem. Phys. **11**, 10543 (2009).
[22] Z. Niu and H. W. Gibson, Chem. Rev. **109**, 6024 (2009).

[23] Q. Wu, P. M. Rauscher, X. Lang, R. J. Wojtecki, J. J. de Pablo, M. J. A. Hore, and S. J. Rowan, Science **358**, 1434 (2017).
[24] P. Rauscher, K. Schweizer, S. Rowan, and J. de Pablo, J. Chem. Phys. **152**, 214901 (2020).
[25] P. M. Rauscher, S. J. Rowan, and J. J. de Pablo, ACS Macro Lett. **7**, 938 (2018).
[26] N. Kanaeda and T. Deguchi, Prog. Theor. Phys. Suppl. **191**, 146 (2011).
[27] A. R. Klotz, B. W. Soh, and P. S. Doyle, Proc. Nat. Acad. Sci. U. S. A. **117**, 121 (2020).
[28] B. W. Soh and P. S. Doyle, ACS Macro Lett. **9**, 944 (2020).
[29] B. A. Krajina, A. Zhu, S. C. Heilshorn, and A. J. Spakowitz, Phys. Rev. Lett. **121**, 148001 (2018).
[30] B. H. Zimm, J. Chem. Phys. **24**, 269 (1956).
[31] H. C. Öttinger, *Stochastic Processes in Polymeric Fluids* (Springer-Verlag, Berlin, 1996).
[32] See Supplemental Material at http://link.aps.org/supplemental/10.1103/PhysRevE.102.032502 for additional mathematical results and simulation details, which includes Refs. [33–35].
[33] A. Alexander-Katz and R. R. Netz, Macromolecules **41**, 3363 (2008).
[34] A. Narros, A. J. Moreno, and C. N. Likos, Macromolecules **46**, 3654 (2013).
[35] A. Y. Grosberg, Phys. Rev. Lett. **85**, 3858 (2000).
[36] J. Rotne and S. Prager, J. Chem. Phys. **50**, 4831 (1969).
[37] H. Yamakawa, J. Chem. Phys. **53**, 436 (1970).
[38] W. Zylka and H. C. Öttinger, J. Chem. Phys. **90**, 474 (1989).
[39] M. Doi and S. Edwards, *The Theory of Polymer Dynamics* (Oxford University Press, New York, 1986).
[40] H. C. Öttinger, J. Chem. Phys. **83**, 6535 (1985).
[41] H. C. Öttinger, J. Chem. Phys. **86**, 3731 (1987).
[42] J. J. Magda, R. G. Larson, and M. E. Mackay, J. Chem. Phys. **89**, 2504 (1988).
[43] T. W. Liu and H. C. Öttinger, J. Chem. Phys. **87**, 3131 (1987).
[44] G. Tsolou, N. Stratikis, C. Baig, P. S. Stephanou, and V. G. Mavrantzas, Macromolecules **43**, 10692 (2010).
[45] J. M. Wiest, S. R. Burdette, T. W. Liu, and R. B. Bird, J. Non-Newtonian Fluid Mech. **24**, 279 (1987).
[46] www.python.org.
[47] https://github.com/pmrauscher/rpbd.
[48] P. M. Rauscher, K. S. Schweizer, S. J. Rowan, and J. J. de Pablo, Macromolecules **53**, 3390 (2020).
[49] Z. Ahmadian Dehaghani, I. Chubak, C. N. Likos, and M. R. Ejtehadi, Soft Matter **16**, 3029 (2020).